

Estimating Vegetation Cover from High-Resolution Satellite Data to Assess Grassland Degradation in the Georgian Caucasus

Author(s): Martin Wiesmair, Hannes Feilhauer, Anja Magiera, Annette Otte, and Rainer Waldhardt

Source: Mountain Research and Development, 36(1):56-65.

Published By: International Mountain Society

DOI: <http://dx.doi.org/10.1659/MRD-JOURNAL-D-15-00064.1>

URL: <http://www.bioone.org/doi/full/10.1659/MRD-JOURNAL-D-15-00064.1>

BioOne (www.bioone.org) is a nonprofit, online aggregation of core research in the biological, ecological, and environmental sciences. BioOne provides a sustainable online platform for over 170 journals and books published by nonprofit societies, associations, museums, institutions, and presses.

Your use of this PDF, the BioOne Web site, and all posted and associated content indicates your acceptance of BioOne's Terms of Use, available at www.bioone.org/page/terms_of_use.

Usage of BioOne content is strictly limited to personal, educational, and non-commercial use. Commercial inquiries or rights and permissions requests should be directed to the individual publisher as copyright holder.

Estimating Vegetation Cover from High-Resolution Satellite Data to Assess Grassland Degradation in the Georgian Caucasus

Martin Wiesmair^{1,3*}, Hannes Feilhauer², Anja Magiera³, Annette Otte^{1,3}, and Rainer Waldhardt³

* Corresponding author: martin.wiesmair@umwelt.uni-giessen.de

¹ Center for International Development and Environmental Research, Justus Liebig University Giessen, Senckenbergstrasse 3, 35390 Giessen, Germany

² Institute of Geography, Friedrich-Alexander University, Wetterkreuz 15, 91058 Erlangen, Germany

³ Division of Landscape Ecology and Landscape Planning, Justus Liebig University, Heinrich-Buff-Ring 26, 35392 Giessen, Germany

© 2016 Wiesmair et al. This open access article is licensed under a Creative Commons Attribution 4.0 International License (<http://creativecommons.org/licenses/by/4.0/>). Please credit the authors and the full source.



In the Georgian Caucasus, unregulated grazing has damaged grassland vegetation cover and caused erosion. Methods for monitoring and control of affected territories are urgently needed.

Focusing on the high-montane and subalpine grasslands of the upper Aragvi Valley, we sampled grassland for soil, rock, and vegetation cover to test the applicability of a site-specific remote-sensing approach to observing grassland degradation. We used random-forest regression to

separately estimate vegetation cover from 2 vegetation indices, the Normalized Difference Vegetation Index (NDVI) and the Modified Soil Adjusted Vegetation Index (MSAVI₂), derived from multispectral WorldView-2 data (1.8 m). The good model fit of $R^2 = 0.79$ indicates the great potential of a remote-sensing approach for the observation of grassland cover. We used the modeled relationship to produce a vegetation cover map, which showed large areas of grassland degradation.

Keywords: Grassland degradation; erosion; overgrazing; NDVI; MSAVI₂; WorldView-2; Georgia; Caucasus.

Peer-reviewed: September 2015 **Accepted:** November 2015

Introduction

Grassland ecosystems provide multiple goods and services such as food products from ruminants, erosion control, and recreation. Globally, vast grassland areas have undergone degradation that has been triggered by the impacts of climate change and anthropogenic activities such as overgrazing (Gang et al 2014). Grassland degradation from overgrazing is common in developing countries, in which local populations suffer from the consequences of degradation such as socioeconomic hardship and increased natural disasters (Liu and Diamond 2005).

Similar processes can be observed in Central Asian and Caucasian countries where a transition in livestock management has taken place (Suttie et al 2005). During the Soviet period, sheep husbandry was practiced with summer grazing in mountain sites and winter grazing in the lowlands. On their migration routes, large sheep herds damaged the vegetation layer of steep slopes (Körner 1980). Nowadays, in most parts of Georgia, migratory sheep husbandry has been replaced by localized cattle farming. Further, in the Georgian Caucasus, erosion is caused by unregulated cattle grazing and logging of

protected forests; both have increasingly negative effects on soil stability (Ministry of Environment Protection et al 2009). To control land degradation, the Georgian national risk assessment report defined areas in the Georgian Caucasus that are prone to natural disasters (CENN and Faculty of Geo Information Science and Earth Observation, University of Twente 2012). Restoration and sustainable use of pastures are urgently required. Furthermore, the growing popularity of hiking and downhill skiing requires sustainable management of sensitive recreational sites.

Approaches to recording the extent of grassland degradation in developing countries have emerged in China, where about 90% of grasslands are considered degraded due to overgrazing and other factors (Liu and Diamond 2005). Akiyama and Kawamura (2007) proposed grassland monitoring by means of remote sensing (RS) as a promising tool for restoring and sustainably managing affected regions. For a long time, the use of RS to monitor arid and semiarid grassland cover has been recognized as essential to determining livestock capacity in order to prevent desertification (Purevdorj et al 1998).

The observation of vegetation cover on a larger scale at multiple time points makes RS approaches beneficial

for monitoring purposes. Liu et al (2005) used RS methods to estimate the vegetation cover of alpine grassland in Qinghai Province in China. Their results showed high accuracy levels, which indicate the applicability of RS methods for mountainous terrain.

Previous studies on the estimation of vegetation cover relied on examinations at a rather coarse spatial resolution of 30 m × 30 m. Such a scale is unlikely to show the heterogeneity of grass cover (Zha et al 2003), as variations occur within a few meters in mountainous terrain (Asner and Lobell 2000). Consequently, there is a need to detect small-scale vegetation damage points, in order to prevent further erosion in mountainous regions (Alewell et al 2008). Increasing the spatial resolution of space-borne sensors broadens RS options; resolution should be chosen in accordance with the spatial scale of the environmental pattern that is analyzed (Feilhauer et al 2013). We chose imagery from WorldView-2, one of the multispectral sensors with the highest available spatial resolution for our area of interest. The applicability of vegetation indices for the estimation of vegetation cover has been tested with field spectrometers and satellite images (Gessner et al 2013; Lehnert et al 2015). From a wide range of vegetation indices, the Normalized Difference Vegetation Index (NDVI) and the Modified Soil Adjusted Vegetation Index (MSAVI₂) have been proposed as good predictors of arid and semiarid grassland vegetation cover (Purevdorj et al 1998; Liu et al 2007).

In this study, we developed a site-specific RS approach to assessing grassland degradation based on vegetation cover. This assessment can inform management of vulnerable grasslands in the upper Aragvi Valley, where grassland degradation, erosion, and mudflows frequently occur. We tested the 2 multispectral vegetation indices MSAVI₂ and NDVI for their appropriateness to detect changes in grassland cover from high-resolution satellite images. To evaluate the indices' ability to assess heterogeneous mountain terrain, we determined the compositional cover values of rock, soil, and vegetation across varying degradation intensities. From the data of the NDVI we mapped the high-montane and subalpine grassland cover for our area of interest.

Methods

Study area

The study was conducted in the upper Aragvi Valley in the vicinity of the village of Mleta in the Greater Caucasus in Georgia (Figure 1). Mleta (42°25'52"N, 44°29'52"E, 1535 m above sea level [masl]) is situated on the Georgian Military Road, which connects Tbilisi, the capital of Georgia, with Russia. Mleta consists of 2 parts, Zvemo (Upper) Mleta and Kvemo (Lower) Mleta. South of Mleta, at the bottom of the upper Aragvi Valley, lies the village of Pasanauri (42°21'8"N, 44°41'16"E, 1050 masl). Climate

data were contributed by the National Environmental Agency and modified by Ina Keggenhoff. The study area has a mean annual temperature of 8.2°C and a mean annual precipitation of 1011 mm. January, the coldest month, has a mean temperature of -3.3°C and 50 mm mean precipitation. The hottest month, July, has a mean temperature of 18.9°C and a mean precipitation of 103 mm.

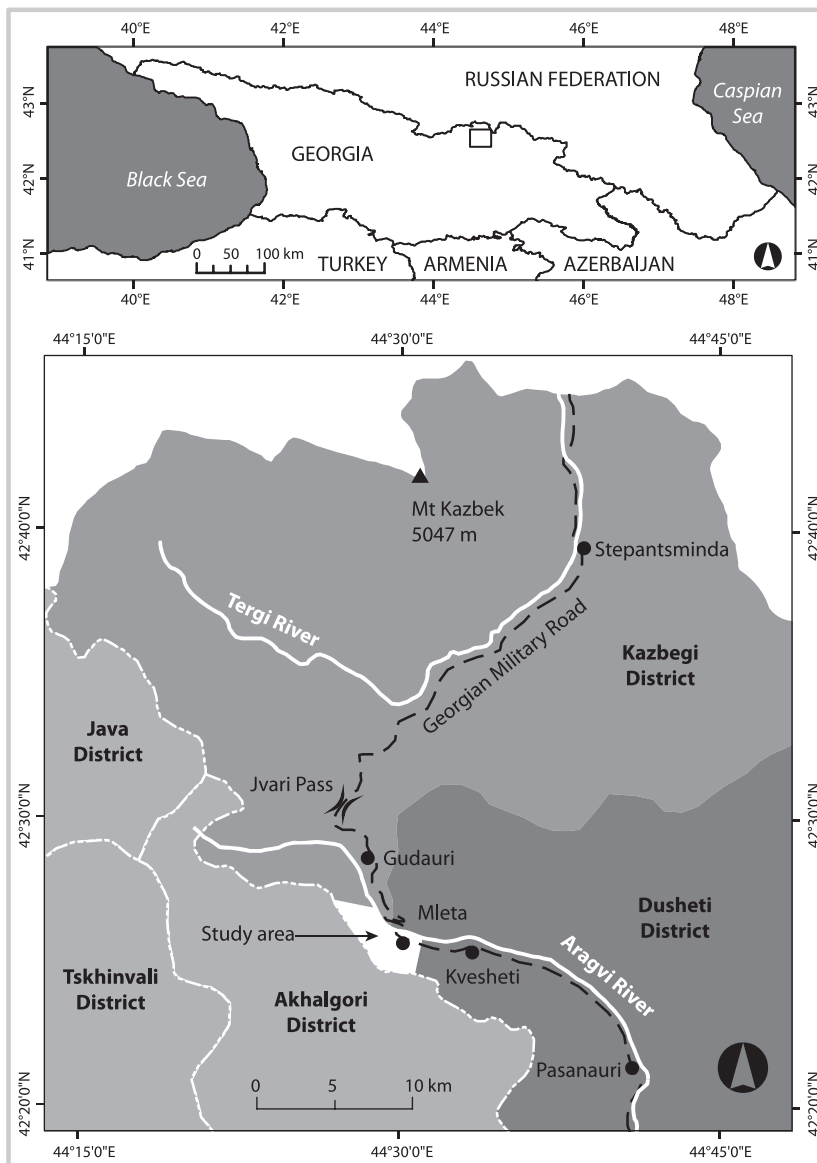
The upper Aragvi Valley is formed by andesite-basalt in alternation with clay shale, shale marls, and enclosures of limestone and sandstone (Khetskhoveli et al 1975; Gobejishvili et al 2011). Close to Mleta, the upper Aragvi Valley is asymmetrically shaped. The slightly inclined, north-facing side is covered by loose sediment, which is prone to erosion and mudflows (Lichtenegger et al 2006). In the Aragvi Valley, mountain meadow and forest soil can be found (Georgian Institute of Public Affairs 2007). According to the World Reference Base for soil (IUSS Working Group WRB 2007), soil types in the mountain meadows include Leptosols, Cambisols, and Cryosols. The mountain forest soil mainly consists of Dystric Cambisol. Along the river valley, alluvial deposits have built up Calcaric Fluvisols.

The slopes near Mleta range from the river valley bottom at approximately 1500 masl to the ridges at about 2200 masl. The north-facing slopes are characterized by beech forests (*Fagus orientalis*), large erosion gullies, and grassland, which is mainly used for cattle grazing. Cattle tracks and erosion can be observed on the steep slopes of the grassland (Figure 2A). Due to anthropogenic impact and topographic features, no clear demarcation line can be drawn between the high-montane and subalpine zones of the Greater Caucasus (Lichtenegger et al 2006; Nakhutsrishvili et al 2006). We defined the high-montane zone border at about 1900 masl, where scattered rhododendron shrubs (*Rhododendron luteum*) indicate a transition to the subalpine zone. The high-montane grassland comprises grass species such as *Agrostis planifolia*, *Cynosurus cristatus*, *Festuca pratensis*, *Poa pratensis*, and *Trisetum flavescens* (Khetskhoveli et al 1975; Lichtenegger et al 2006). The subalpine grassland is characterized by *Astrantia maxima*, *Betonica macrantha*, *Festuca varia*, *Inula orientalis*, and a strong infestation of *Veratrum lobelianum* (Figure 2C).

Field data

In July 2012 and 2013, we sampled plots (25-m²) of high-montane and subalpine grassland for vegetation cover, soil cover, and rock cover. In our study area, July is the month of peak plant development; thus, that period offered ideal conditions for vegetation sampling. In the plots, we arranged three 1 m² subplots in a triangle with the tip aligned uphill (Figure 3). We selected plots according to their total vegetation cover to sample a gradient of grassland coverage. All plots were located on the slope; the flat terrain was not sampled.

FIGURE 1 Map of the study area and its location within the Caucasus region. (Map by Martin Wiesmair)



Vegetation and soil cover are essential indicators of grassland health or degradation (Zhang et al 2013). Therefore, we visually estimated the percentages of vegetation, soil, and rock cover. However, due to observer estimation error, the vegetation cover estimates did not yield satisfying model results. To increase accuracy, we photographed the ground vegetation cover and further used these digital images to determine vegetation cover. Therefore each subplot was photographed with a handheld digital camera (Panasonic LUMIX DMC-TZ1, 5 Megapixel). Photos were taken from a distance to the canopy height over plain ground at nadir 140 cm. We used the image processing program Photoshop CS5 version 12 (Adobe Systems, Mountain View, CA) to

calculate the vegetation cover of each subplot. Within each subplot image, we identified pixels that represented vegetation and used the ratio of vegetation pixels to total image pixels to define the percentage of vegetation cover. We further distinguished between the covers of vascular plants and mosses, as mosses considerably contribute to the greenness of sparsely vegetated terrain (Karnieli et al. 2002, 1996). Finally, the plot vegetation cover was computed from the mean of the embedded subplot values calculated before. Altogether, 5 plots were detected as outliers and were removed from further analysis. The remaining 93 plots were then grouped into 4 classes of degradation intensity, based on their percentage of vegetation cover (Table 1), a classification comparable to

FIGURE 2 Grassland of the upper Aragvi Valley. (A) Cattle tracks and erosion from grazing on steep slopes near the villages; (B) cattle grazing on nondegraded, high-montane grassland; (C) subalpine grassland with an infestation of *Veratrum lobelianum*; (D) grassland degradation along a hiking trail. (Photos by Martin Wiesmair)



those used in other studies. We used the Wilcoxon rank sum test with Bonferroni correction method for post-hoc class comparisons. All analyses were performed using the R Project statistical computing software (R Core Team 2014).

To extract spectral information from the satellite image, we sampled the geographic position of each plot. The 4 coordinates of our plot corners were recorded with a GPS device (Garmin GPSMap 62s) with a 3–5 m position accuracy. To increase geographic position accuracy, we repeated positioning on a different date, marking plot centers with magnetic markers to locate the plots with a metal detector (Figure 3). We further used the mean center function of ArcGIS10 (ESRI, Redlands, CA) to compute the geographic mean of 8 GPS points for each plot.

Multispectral data and analysis

We chose the WorldView-2 satellite sensor, which provides 8 spectral bands from visible (400 nm) to near-infrared (1040 nm) at a spatial resolution of 1.84 m. The sensor provides a radiometric resolution of 11 bit and 16.4 km swath width with a revisiting time of 3.7 days (Digitalglobe 2013). Compared to other satellite sensors, WorldView-2 offers a very high spatial resolution

(Ünsalan and Boyer 2011). Recently launched sensors such as WorldView-3 have an even higher spatial resolution but were not yet available when our studies took place. Our WorldView-2 image was acquired on 8 July 2011, during the period of highest vegetation density. The image was atmospherically corrected with the ATCOR 2 module of ERDAS 2013 (DLR, Wessling, Germany).

The vegetation indices MSAVI₂ and NDVI were calculated for our plots from the satellite image following Equations 1 and 2:

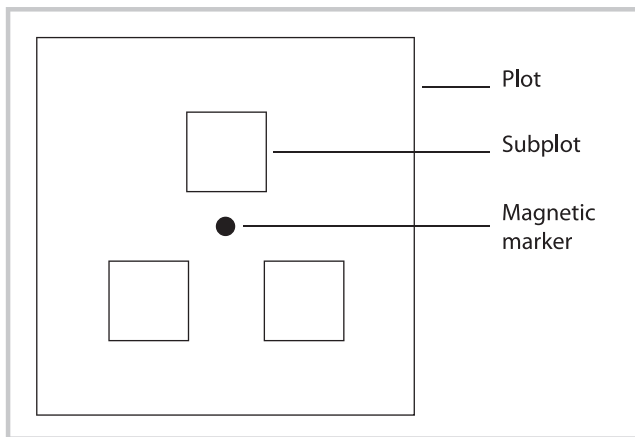
$$MSAVI_2 = \left(2r_{NIR} + 1 - \sqrt{(2r_{NIR} + 1)^2 - 8(r_{NIR} - r_{RED})} \right) / 2, \quad (1)$$

$$NDVI = \frac{r_{NIR} - r_{RED}}{r_{NIR} + r_{RED}} \quad (2)$$

where r_{NIR} and r_{RED} are the simulated reflectance values in near-infrared and red.

We used NDVI and MSAVI₂ separately as predictors for vegetation cover in our random-forest regression analyses. The random-forest approach has been successfully used to analyze RS data (Lawrence et al 2006; Rodriguez-Galiano et al 2012; Feilhauer et al 2014). From

FIGURE 3 Arrangement of subplots and magnetic marker.



the R-package “randomForest 4.6-7” (Liaw and Wiener 2002; Breiman and Cutler 2012) we chose the default setting for the number of predictors sampled for the splitting at each node. As suggested by Breiman (2003), we tested other values, but the default parameterization produced the best results. The number of trees to grow was set to 5000.

We used 100 times bootstrapping with replacement to validate the data sample. A predicted vegetation cover value for each plot was calculated from the mean of each bootstrap sample. The random-forest model fit was validated through a linear regression of the predicted versus the observed (ground truth) values. For each model we calculated the total root mean square error of prediction (RMSEP), a commonly used criterion for judging the performance of a multivariate calibration model (Faber 1999). For comparisons to other studies, we additionally extracted the RMSEP of each degradation class. All analyses were based on the continuous vegetation cover range. Afterward the classification levels were applied to the model results. The RMSEP was calculated following Equation 3:

$$RMSEP = \sqrt{\sum_{i=0}^n \left((X_i - Y_i)^2 / n \right)} \quad (3)$$

where X is the predicted value from the model, Y the observed value, and n the number of predictions.

A grassland vegetation cover map was predicted from NDVI values, which were extracted from the WorldView-2 satellite image. We applied a continuous vegetation cover scale to a map, where we masked out larger forested areas, streams, clouds, the Aragvi River bed, and settlements.

Results

Grassland management

During our fieldwork, we witnessed the grassland management of the upper Aragvi Valley. Grassland is

TABLE 1 Classification of degradation intensity of Georgian high-montane and subalpine grassland based on vegetation cover (modified from Purevdorj et al 1998, Gao et al 2006, and Liu et al 2007).

Vegetation cover (%)	Degradation class
80–100	None
60–79	Light to moderate
30–59	Moderate to severe
0–29	Extreme

commonly used by all village inhabitants, mainly for cattle grazing on all vegetation cover densities. Most of the grassland area was used as pasture; only small parcels of meadows were fenced off to exclude grazing animals. In order to make use of the whole grassland area, some of the cattle remained close to the villages while others were driven to nearby grazing grounds each morning (Figure 2B). The cattle roamed freely during the day and returned to the village in the evening. Small herds of free-roaming horses were met on plateaus with dense vegetation cover. We observed controlled sheep herding on distant pastures southeast of Mleta near the village of Kvesheti. The hiking trails leading to a monastery on top of the mountain range attracted many tourists and pilgrims. The trails lie within the grassland, and we detected severe vegetation damage spots along them (Figure 2D). Minor work to restore parts of one hiking trail has been undertaken.

Site cover variables and vegetation cover models

Site variables are displayed as median values for each degradation class in Table 2. Soil cover ranged from 4 to 24% and rock cover from 0 to 50%. The soil and rock cover were lowest in sites of no degradation and highest in extremely degraded sites. All classes differed significantly, except that the soil cover of moderately to severely degraded sites did not differ from that of light to moderately degraded and extremely degraded sites. Soil and rock cover were strongly negatively correlated with vegetation cover.

Table 3 displays the validated results of both random-forest regression models with corresponding model errors within vegetation cover classes. The validation was calculated from bootstrapped predicted versus observed data. Values for each vegetation cover class were extracted from the model results, which were previously run from the full range of vegetation cover. NDVI and MSAVI₂ were calculated from a WorldView-2 satellite image. To visualize the model fits, we plotted values predicted by the model versus the observed values (Figure 4). We observed identical model fits for both vegetation indices at $R^2 = 0.79$. Minor differences in total errors or errors of individual degradation classes were observed between NDVI and MSAVI₂. The RMSEP for MSAVI₂ was 0.02% cover higher on severely and nondegraded classes. For extremely degraded sites, MSAVI₂ was 0.11% cover higher than NDVI and did not differ on moderately degraded sites. With

TABLE 2 Median values of environmental variables for each degradation intensity class.

Environmental variable	Degradation class				R^e
	None	Light to moderate	Moderate to severe	Extreme	
Vegetation cover (%)	91.5	70.2	42.2	23.7	–
Soil cover (%)	4.0 ^{a)}	12.5 ^{a),b)}	20.0 ^{b),c)}	24.0 ^{c)}	–0.73
Rock cover (%)	0.0 ^{a)}	8.0 ^{b)}	31.5 ^{c)}	50.0 ^{d)}	–0.87

^{a),b),c),d)}Significant variable differences for the Wilcoxon rank sum test of a post-hoc cluster comparison using the Bonferroni correction method ($P < 0.05$).

^{e)}Spearman correlation coefficient of vegetation cover to soil and rock cover at $P < 0.05$.

decreasing vegetation cover, the model error increased for both indices.

We found the largest proportions of grassland degradation within the high-montane zone (Figure 5). Through visual interpretation we identified errors that corresponded to the given RMSEP values of about 15% cover on the extremely degraded sites, which are attributed to erosion gullies and zones of accumulation of debris flow.

Discussion

Grassland management

Our vegetation cover map indicates a higher pressure of cattle grazing on pastures near the village of Mleta, where we found more degraded areas. Similar developments have been observed within other former Soviet countries in Central Asia (Iniguez et al 2005). As the animals remain longer in nearby areas, these grasslands are more intensively grazed (Suttie et al 2005). In addition to land use, topographical conditions affect the severity of erosion. Tasser et al (2003) found that a slope inclination of 30–40% increased the risk of alpine grassland erosion in the Alps. Therefore, steep slopes near villages can be considered to be of higher risk for grassland degradation. Slope inclination was not considered in our model but should be incorporated in future management plans.

The weeds *Veratrum lobelianum* and *Cirsium obvallatum*, which have been reported in grazing areas in the Caucasus (Callaway et al 2000), primarily occur in the subalpine zone in areas with dense vegetation cover.

Therefore, the influence of varying spectral characteristics of grazing weeds, as has been proposed by Liu et al (2015), is mainly restricted to the subalpine zone. The subalpine zone of the study region is further interspersed with rhododendron shrubs, which might further contribute to variation in the spectral characteristics of dense vegetation cover. Nevertheless, the degradation spots along the hiking trails are well displayed on our vegetation cover map for the subalpine zone.

Vegetation cover assessment

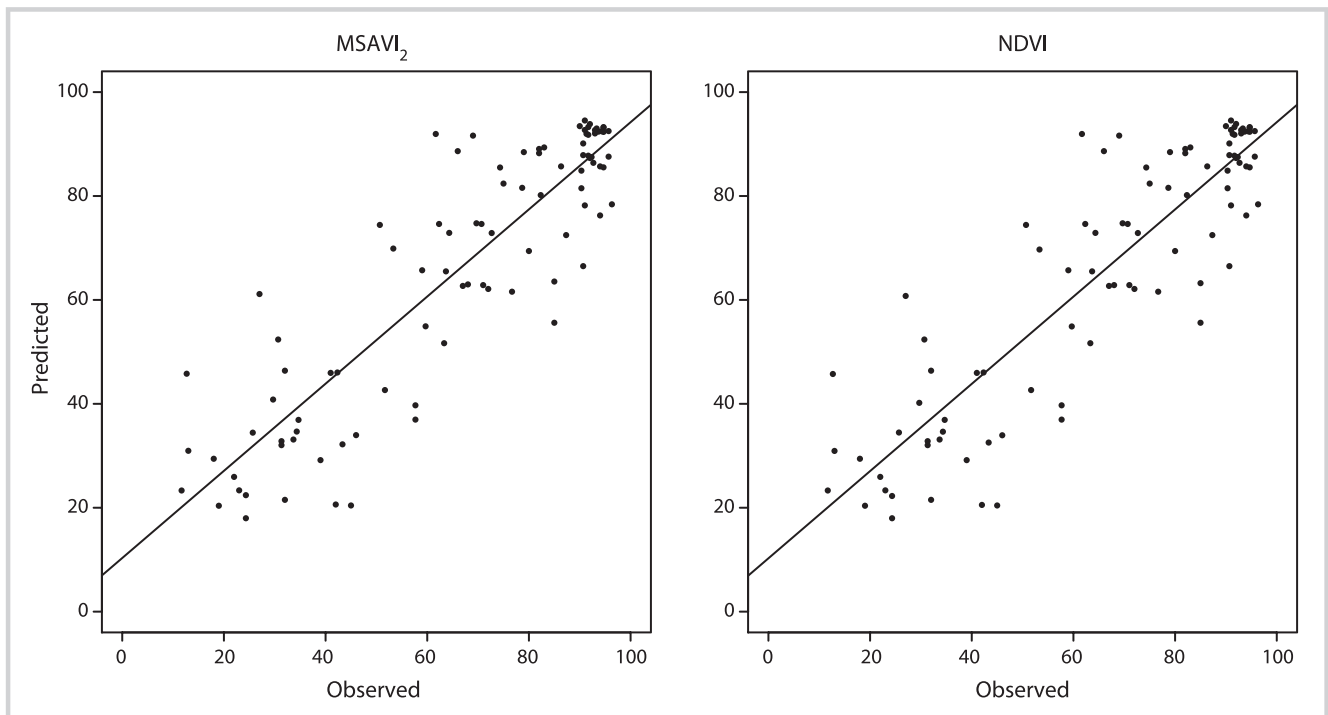
Grassland in the study region showed higher proportions of soil and rock cover with increasing degradation intensity. This is in accordance with described erosion processes on steep slopes of the Alps. First, the vegetation layer is damaged, and then clods of soil are washed downward until the base rock layer becomes exposed (Stahr 1997). Although revegetation can be observed to some extent on these extremely degraded sites, the natural formation of a new soil layer on degraded mountain slopes is an extremely slow process.

Considering the differing site coverages of our study region, the differences in the spectral reflectance of rock, soil, and vegetation have to be considered for RS methods (Elvidge and Lyon 1985; Clark 1999). Purevdorj et al (1998) showed that MSAVI₂ produced fewer errors than NDVI in the estimation of very low vegetation cover. In our model, differences between NDVI and MSAVI₂ were negligible, which is most likely attributable to different site conditions: Sampling plots in our study area included

TABLE 3 Validated model fit of random forest regression models.

Vegetation index	R^2	RMSEP				
		Extreme degradation	Moderate to severe degradation	Light to moderate degradation	No degradation	Total
NDVI	0.79	16.11	14.25	13.29	9.81	12.61
MSAVI ₂	0.79	16.22	14.27	13.29	9.79	12.63

FIGURE 4 Model fits for NDVI and MSAVI₂ based on predicted and observed vegetation cover values, given as percentage.



steep slopes up to 43° inclination, and the soil cover values did not exceed those for vegetation or rock cover. It is possible that the stronger topographic influence and high rock cover values interfered with the MSAVI₂, which therefore did not mitigate the soil background effect and did not strongly differ from NDVI. The similarity between the 2 vegetation indices at high vegetation cover has also been demonstrated by Qi et al (1994). Furthermore, both indices were found to be strongly influenced by variations in spectral signals of rock–soil brightness (Elvidge and Lyon 1985).

Considering our model errors and map interpretation, the high rock cover within erosion gullies is most likely causing the higher errors in the prediction of vegetation cover < 30%. Even though Liu et al (2007) and Purevdorj et al (1998) showed high model accuracies for vegetation cover < 30%, our results indicate restricted applicability of the vegetation indices for very high rock covers in mountainous terrain. Novel approaches for grassland monitoring by means of multispectral reflectance incorporate several vegetation indices and performed well on the Tibetan plateau (Lehnert et al 2015). Topographic correction methods, an incorporation of further vegetation indices, and advanced regression methods such as the support vector machine, which were presented by Lehnert et al (2015), might further improve model results.

Our model's error rate is comparable to that of visual field interpretations, which can range from 10% (Kennedy and Addison 1987) to 15–40% (Tonteri 1990).

We assume that the NDVI's high sensitivity to changes in vegetation cover enabled the good model results. In our study, NDVI derived from multispectral reflectance was shown to detect grassland degradation at a high spatial resolution of 1.84 m, which seems to be appropriate to detect small vegetation damage spots in heterogeneous grassland terrain.

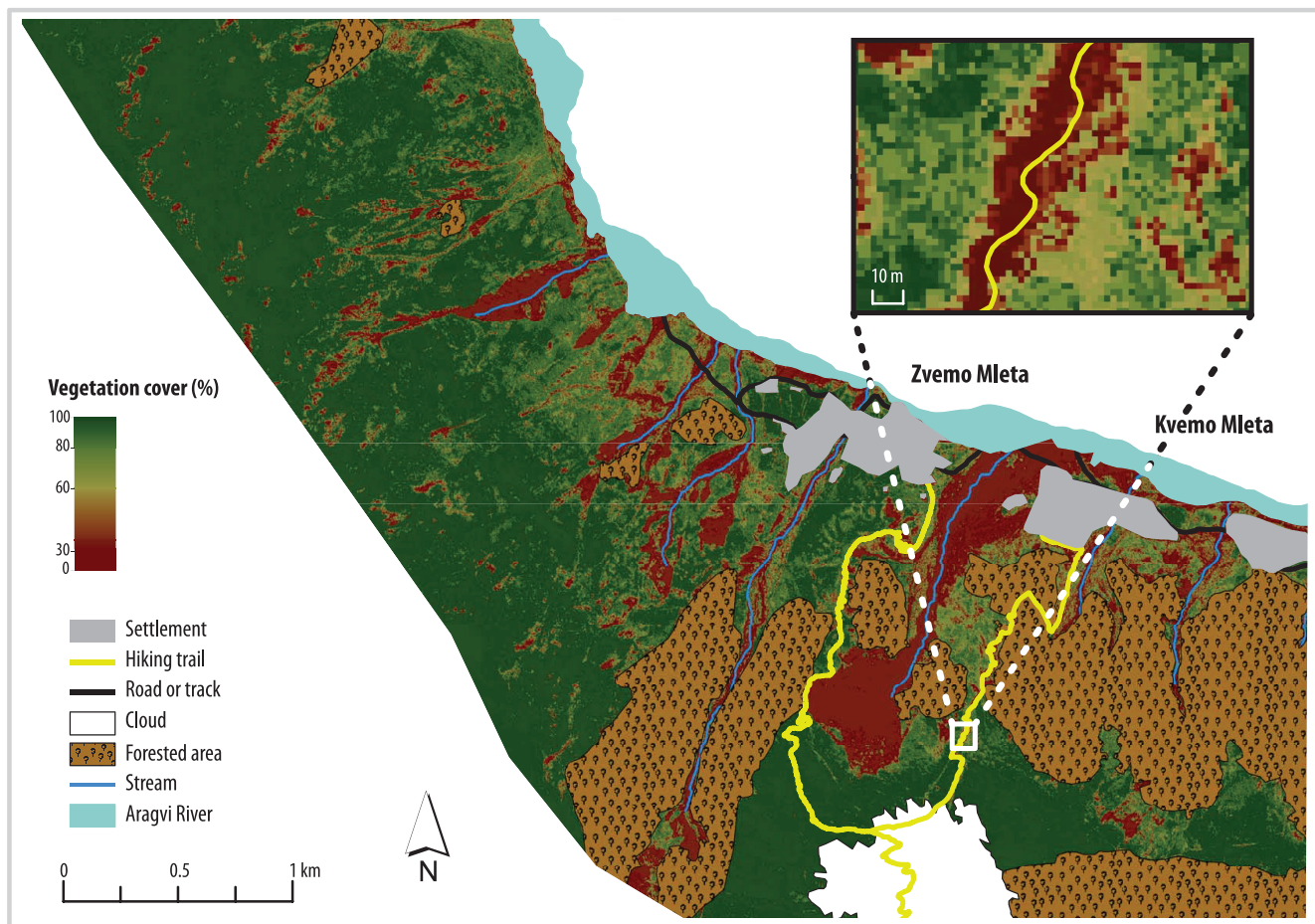
Practical implications

Our models proved to be most suitable for mapping vegetation cover of 30–100%. To control erosion in high-montane grassland, vegetation cover of at least 70% is needed (Moismann 1984). Therefore, our models' coverage range is of highest interest for early detection of grassland degradation to enable the implementation of appropriate grazing management and restoration practices.

The manual classification of vegetation cover from photographs of ground cover was highly time consuming, and automated classification methods have been presented as time-saving alternatives by other authors (eg Vanha-Majamaa et al 2000; Zhou and Robson 2001). Although novel methods to retain the fractional vegetation cover from satellite images have been developed (eg Li et al 2014), monitoring should always be supported by field surveys (Gintzburger and Saidi 2010).

Regarding the satellite acquisition date, our model results proved that the period of optimum vegetation growth is an appropriate time to differentiate vegetation

FIGURE 5 Vegetation cover predicted by NDVI for a high-montane and subalpine grassland in the upper Aragvi Valley in 2011. Inset shows degradation along a hiking trail. (Map by Martin Wiesmair)



cover from soil and rock cover. This has also been demonstrated for other regions with highest separability of green vegetation cover from soil/rock cover (Dennison and Roberts 2003; Marsett et al 2006; Feilhauer and Schmidtlein 2011).

Because of their cost, WorldView-2 images can generally be applied only to small areas. Their use in transitional and developing countries can be limited to areas near villages that have been defined as vulnerable by larger assessments (such as the Georgian national risk assessment—CENN and Faculty of Geo Information Science and Earth Observation, University of Twente 2012), skiing slopes, and intensively used hiking trails.

For mountainous areas, general assumptions about grassland degradation based on vegetation cover should only be made after incorporating local knowledge about land use. For the upper Aragvi Valley, the loss of vegetation cover from land use and erosion has been well described (eg Khetskhoveli et al 1975; Körner 1980; Lichtenegger et al 2006). Additional impacts of overgrazing include reduction of plant diversity and infestation by unpalatable weed species (Liu et al 2004).

In the upper Aragvi Valley, these additional types of grassland degradation can be observed. This study, however, focused exclusively on loss of total vegetation cover. Its interrelationship with other degradation types was not tested in the study and would be a fruitful avenue for further research.

Conclusion

Transitional countries like Georgia have experienced substantial changes in land use, agricultural systems, and the tourism industry. Further development needs to take place in an environmentally sustainable manner. In order to reduce grassland degradation caused by uncontrolled grazing, the establishment of case-related, sustainable grazing management adapted to the vulnerable mountain grassland is urgently needed.

In the upper Aragvi Valley, the severe grassland degradation near the village of Mleta indicates that the local population is threatened by mass wasting events and the loss of available grazing grounds, and management measures are therefore necessary to

prevent these risks. While the extremely degraded slopes require substantial revegetation efforts, more moderately degraded areas might be restored by better-regulated cattle grazing. In using RS to estimate grassland cover, uncertainties due to changes in plant composition and background signals have to be considered. Nevertheless, the RS method presented here can be used to detect changes in vegetation cover with an error rate that is comparable to the error rate of on-site field observations.

We propose the following site-specific management measures for the upper Aragvi Valley and mountain regions that face similar environmental problems:

- Take into account the whole range of vegetation cover.
- Accompany RS monitoring with field observations.
- Take information on slope inclination into account.

Maps of vegetation cover produced in the presented way can play a key role in the evaluation of current grassland degradation, the decision for potential tourist development, and the success of future management plans.

ACKNOWLEDGMENTS

This study contributes to the framework of the major project “Analyzing multiple interrelationships of environmental and societal processes in mountainous regions of Georgia (AMIES),” funded by the Volkswagen Foundation. The German Academic Exchange Service (DAAD) partly funded fieldwork in Georgia. We thank our

Georgian colleagues George Nakhutsrishvili, Maia Akhalkatsi, Otar Abdaladze, and Giorgi Mikeladze. We also thank Zevva Asanidze, Nato Tephnadze, and Luka Tarielashvili for their fieldwork assistance. Finally, we thank the National Environmental Agency and Ina Keggenhoff for providing the climate data.

REFERENCES

- Akiyama T, Kawamura K.** 2007. Grassland degradation in China: Methods of monitoring, management and restoration. *Grassland Science* 53:1–17.
- Alewel C, Meusburger K, Brodbeck M, Bänninger D.** 2008. Methods to describe and predict soil erosion in mountain regions. *Landscape and Urban Planning* 88:46–53.
- Asner GP, Lobell DB.** 2000. A biogeophysical approach for automated SWIR unmixing of soils and vegetation. *Remote Sensing of Environment* 74:99–112.
- Breiman L.** 2003. Manual on setting up, using, and understanding random forests v4.0. http://oz.berkeley.edu/users/breiman/Using_random_forests_v4.0.pdf; accessed on 19 December 2014.
- Breiman L, Cutler A.** 2012. Random forests. <https://www.stat.berkeley.edu/~breiman/RandomForests/>; accessed on 19 December 2014.
- Callaway RM, Kikvidze Z, Kikodze D.** 2000. Facilitation by unpalatable weeds may conserve plant diversity in overgrazed meadows in the Caucasus Mountains. *Oikos* 89:275–282.
- CENN [Caucasus Environmental NGO Network], Faculty of Geo Information Science and Earth Observation, University of Twente.** 2012. *Atlas of Natural Hazards and Risks of Georgia*. Tbilisi, Georgia: Caucasus Environmental NGO Network and University of Twente. Also published online at http://issuu.com/grammaltic/docs/atlas_of_risk; accessed on 19 December 2014.
- Clark RN.** 1999. Spectroscopy of rocks and minerals, and principles of spectroscopy. In: Rencz AN, editor. *Manual of Remote Sensing. Remote Sensing for the Earth Sciences*. 3rd edition. Vol. 3. New York, NY: John Wiley and Sons, pp 3–58.
- Dennison PE, Roberts DA.** 2003. The effects of vegetation phenology on endmember selection and species mapping in southern California chaparral. *Remote Sensing of Environment* 87:295–309.
- Digitalglobe.** 2013. *Datasheet World View 2*. <https://www.digitalglobe.com/resources/satellite-information>; accessed on 17 December 2015.
- Elvidge CD, Lyon RJP.** 1985. Influence of rock-soil spectral variation on the assessment of green biomass. *Remote Sensing of Environment* 17:265–279.
- Faber N.** 1999. Estimating the uncertainty in estimates of root mean square error of prediction: Application to determining the size of an adequate test set in multivariate calibration. *Chemometrics and Intelligent Laboratory Systems* 49:79–89.
- Feilhauer H, Dahlke C, Doktor D, Lausch A, Schmidtlein S, Schulz G, Stenzel S.** 2014. Mapping the local variability of Natura 2000 habitats with remote sensing. *Applied Vegetation Science* 17:765–779.
- Feilhauer H, Schmidtlein S.** 2011. On variable relations between vegetation patterns and canopy reflectance. *Ecological Informatics* 6:83–92.
- Feilhauer H, Thonfeld F, Faude U, He KS, Rocchini D, Schmidtlein S.** 2013. Assessing floristic composition with multispectral sensors—A comparison based on monotemporal and multiseasonal field spectra. *International Journal of Applied Earth Observation and Geoinformation* 21:218–229.
- Gang C, Zhou W, Chen Y, Wang Z, Sun Z, Li J, Qi J, Odeh I.** 2014. Quantitative assessment of the contributions of climate change and human activities on global grassland degradation. *Environmental Earth Sciences* 72:4273–4282.
- Gao Q, Li Y, Wan Y, Lin E, Xiong W, Jiangcun W, Wang B, Li W.** 2006. Grassland degradation in Northern Tibet based on remote sensing data. *Journal of Geographical Sciences* 16:165–173.
- Georgian Institute of Public Affairs.** 2007. Characterization of soils. http://agromarket.ge/soil_maps/niadagebis_daxasiateba.shtml; accessed on 19 December 2014.
- Gessner U, Machwitz M, Conrad C, Dech S.** 2013. Estimating the fractional cover of growth forms and bare surface in savannas. A multi-resolution approach based on regression tree ensembles. *Remote Sensing of Environment* 129:90–102.
- Gintzburger G, Saidi S.** 2010. From inventory to monitoring in semi-arid and arid rangelands. In: Squires V, editor: *Range and Animal Sciences and Resource Management*. Vol. II. Oxford, United Kingdom: Encyclopedia of Life Support Systems (EOLSS); pp 237–273.
- Gobejishvili R, King L, Lomidze N, Keller T, Tielidze L, Polenthon I.** 2011. *Relief and Geodynamic Processes of High Mountainous Region of Caucasus (Stepantsminda region)*. Collected Papers Report No 3(82). Tbilisi, Georgia: Ivane Javakishvili Tbilisi State University, Vakhushti Bagrationi Institute of Geography.
- Iniguez L, Sulaimenov M, Yusupov S, Ajbekov A, Kineev M, Kheremov S, Abdusattarov A, Thomas D, Musaeva M.** 2005. Livestock Production in Central Asia: Constraints and Opportunities. *ICARDA Caravan* 22:18–22.
- IUSS [International Union of Soil Science] Working Group WRB [World Reference Base].** 2007. *World Reference Base for Soil Resources 2006, First Update 2007*. FAO World Soil Resources Reports Report No 103. Rome, Italy: Food and Agriculture Organization of the United Nations.
- Karnieli A, Gabai A, Ichoku C, Zaady E, Shachak M.** 2002. Temporal dynamics of soil and vegetation spectral responses in a semi-arid environment. *International Journal of Remote Sensing* 23:4073–4087.
- Karnieli A, Shachak M, Tsoar H, Zaady E, Kaufman Y, Danin A, Porter W.** 1996. The effect of microphytes on the spectral reflectance of vegetation in semiarid regions. *Remote Sensing of Environment* 57:88–96.
- Kennedy KA, Addison PA.** 1987. Some considerations for the use of visual estimates of plant cover in biomonitoring. *Journal of Ecology* 75:151–157.
- Khetskhovelii NN, Kharadze AL, Ivanishvili MA, Gagnidze R.** 1975. *Botanical Description of the Georgian Military Road (Tbilisi–Kazbegi–Ordjonikidze)*. Leningrad, Russia: Academy of Sciences of the Georgian SSR, Institute of Botany.
- Körner C.** 1980. Ökologische Untersuchungen an Schafweiden im Zentralkaukasus. *Alm-Bergbauer* 5:151–161.
- Lawrence RL, Wood SD, Sheley RL.** 2006. Mapping invasive plants using hyperspectral imagery and Breiman Cutler classifications (randomForest). *Remote Sensing of Environment* 100:356–362.
- Lehnert LW, Meyer H, Wang Y, Miede G, Thies B, Reudenbach C, Bendix J.** 2015. Retrieval of grassland plant coverage on the Tibetan Plateau based

- on a multi-scale, multi-sensor and multi-method approach. *Remote Sensing of Environment* 164:197–207.
- Li F, Chen W, Zeng Y, Zhao Q, Wu B.** 2014. Improving estimates of grassland fractional vegetation cover based on a pixel dichotomy model: A case study in Inner Mongolia, China. *Remote Sensing* 6:4705–4722.
- Liaw A, Wiener M.** 2002. Classification and regression by randomForest. *R News* 2(3):18–22.
- Lichtenegger E, Bedoschwilli D, Hübl E, Scharfetter E.** 2006. Höhenstufengliederung der Grünlandvegetation im Zentralkaukasus. *Verhandlungen der Zoologisch-Botanischen Gesellschaft in Österreich* 143:43–81.
- Liu B, You G, Li R, Shen W, Yue Y, Lin N.** 2015. Spectral characteristics of alpine grassland and their changes responding to grassland degradation on the Tibetan Plateau. *Environmental Earth Sciences* 74:2115–2123.
- Liu J, Diamond J.** 2005. China's environment in a globalizing world. *Nature* 435:1179–1186.
- Liu Y, Zha Y, Gao J, Ni S.** 2004. Assessment of grassland degradation near Lake Qinghai, West China, using Landsat TM and *in situ* reflectance spectra data. *International Journal of Remote Sensing* 25:4177–4189.
- Liu YS, Hu YC, Peng LY.** 2005. Accurate quantification of grassland cover density in an alpine meadow soil based on remote sensing and GPS. *Pedosphere* 15:778–783.
- Liu Z-Y, Huang J-F, Wu X-H, Dong Y-P.** 2007. Comparison of vegetation indices and red-edge parameters for estimating grassland cover from canopy reflectance data. *Journal of Integrative Plant Biology* 49:299–306.
- Marslett RC, Qi J, Heilman P, Biedenbender SH, Watson MC, Amer S, Weltz M, Goodrich D, Marslett R.** 2006. Remote sensing for grassland management in the arid southwest. *Rangeland Ecology & Management* 59:530–540.
- Ministry of Environment Protection, Natural Resources of Georgia, UNDP Country Office.** 2009. *Georgia's Second National Communication to the UNFCCC*. Tbilisi. <http://unfccc.int/resource/docs/natc/geonc2.pdf>; accessed on 19 December 2014.
- Moismann T.** 1984. Das Stabilitätspotential alpiner Geoökosysteme gegenüber Bodenstörungen durch Skipistenbau. *Verhandlungen der Gesellschaft für Ökologie*:167–176.
- Nakhutsrishvili G, Abdaladze O, Akhalkatsi M.** 2006. Biotope types of the treeline of the central greater Caucasus. In: Gafta DD, Akeroyd DJ, editors. *Nature Conservation*. Environmental Science and Engineering. Berlin, Germany: Springer, pp 211–225.
- Purevdorj T, Tateishi R, Ishiyama T, Honda Y.** 1998. Relationships between percent vegetation cover and vegetation indices. *International Journal of Remote Sensing* 19:3519–3535.
- Qi J, Chehbouni A, Huete AR, Kerr YH, Sorooshian S.** 1994. A modified soil adjusted vegetation index. *Remote Sensing of Environment* 48:119–126.
- R Core Team.** 2014. *R: A Language and Environment for Statistical Computing*. Vienna, Austria: R Foundation for Statistical Computing.
- Rodríguez-Galiano VF, Ghimire B, Rogan J, Chica-Olmo M, Rigol-Sánchez JP.** 2012. An assessment of the effectiveness of a random forest classifier for land-cover classification. *ISPRS Journal of Photogrammetry and Remote Sensing* 67:93–104.
- Stahr A.** 1997. *Bodenkundliche Aspekte der Blaikenbildung auf Almen. Untersuchungen zur Genese von Blattanbrüchen in schluffreichen Almböden*. Forschungsbericht 39. Berchtesgaden, Germany: Nationalparkverwaltung.
- Suttie JM, Reynolds SG, Batello C, Food and Agriculture Organization of the United Nations, editors.** 2005. *Grasslands of the World*. Plant production and protection series. Rome, Italy: Food and Agricultural Organization of the United Nations.
- Tasser E, Mader M, Tappeiner U.** 2003. Effects of land use in alpine grasslands on the probability of landslides. *Basic and Applied Ecology* 4:271–280.
- Tonteri T.** 1990. Inter-observer variation in forest vegetation cover assessments. *Silva Fennica* 24:189–196.
- Ünsalan A, Boyer PKL.** 2011. Remote sensing satellites and airborne sensors. In: Ünsalan A, Boyer PKL, editors. *Multispectral Satellite Image Understanding. From Land Classification to Building and Road Detection*. New York, NY: Springer, pp 7–15.
- Vanha-Majamaa I, Salemaa M, Tuominen S, Mikkola K.** 2000. Digitized photographs in vegetation analysis—A comparison of cover estimates. *Applied Vegetation Science* 3:89–94.
- Zha Y, Gao J, Ni S, Liu Y, Jiang J, Wei Y.** 2003. A spectral reflectance-based approach to quantification of grassland cover from Landsat TM imagery. *Remote Sensing of Environment* 87:371–375.
- Zhang X, Liao C, Li J, Sun Q.** 2013. Fractional vegetation cover estimation in arid and semi-arid environments using HJ-1 satellite hyperspectral data. *International Journal of Applied Earth Observation and Geoinformation* 21:506–512.
- Zhou Q, Robson M.** 2001. Automated rangeland vegetation cover and density estimation using ground digital images and a spectral-contextual classifier. *International Journal of Remote Sensing* 22:3457–3470.